International Journal of Pharmacy and Pharmaceutical Sciences

ISSN- 0975-1491 Vol 9, Issue 11, 2017

Original Article

INDUCTION OF APOPTOSIS BY FATTY ACID RICH FRACTION OF *SOLANUM NIGRUM* ON CERVICAL CANCER CELL LINES

SUBHABRATA PAUL[1*], RITA KUNDU[1#]

[1]Center of Advanced Study, Department of Botany, University of Calcutta, Kolkata 700019, India
[#]Email: kundu_rita@yahoo.co.in

Received: 26 Jul 2017 Revised and Accepted: 21 Sep 2017

ABSTRACT

Objective: Mechanism of cell death inducing pathway of chloroform fraction of methanolic extract of *Solanum nigrum* were studied in a panel of cervical cancer cell line.

Methods: Cells were treated with IC50 doses (previously determined by MTT assay), and various experiments were performed. For cellular and nuclear morphology, cells were stained with Hoechst33258 and observed under phase and fluorescence microscopy. Cell cycle shift and apoptotic assay (AnnexinV-FITC/PI) were studied by flow cytometry. Expressions of relevant genes were studied at the transcriptional and translational levels. ROS induction and loss of MMP and presence of γH2AX were studied by fluorescent microscopy. Constituents of the fraction were separated by column chromatography and bioassayed by MTT assay. Bioactive sub-fractions were identified by GC-MS.

Results: Typical apoptotic morphological features were found in the treated cells. Most cells were found in late apoptotic stages. In HeLa and C33A cell lines, cells were blocked at G1/S, in SiHa, subG0 population increased. Expression of antiapoptotic Bcl-2 decreased and that of proapoptotic BAX, p53, p21 increased. Expression of HPV16 and human ET1 also decreased. ROS mediated DNA damage was detected and induced apoptosis. Different fatty acids along with other compounds were detected in the chloroform fraction, all of which are reported to have anticancer properties.

Conclusion: From the study it can be concluded that fatty acid rich chloroform fraction of *S. nigrum* is capable of inducing apoptosis in cervical cancer cells, through ROS mediated DNA damage**.**

Keywords: Apoptosis, DNA damage, ROS, p53, *Solanum nigrum,* HeLa, SiHa, C33A

DOI: http://dx.doi.org/10.22159/ijpps.2017v9i11.21628

INTRODUCTION

Solanum nigrum commonly known as black nightshade is an erect annual herb. Though the plant is native to Africa, it is found widely throughout the Indian peninsula. In Ayurveda medicine, the plant is considered as an important medicinal herb, having antiseptic and anti-inflammatory properties. The plant is used as diuretic, diaphoretic, anodyne and expectorant. The whole plant is used to treat and cure several ailments such as fever, dropsy, asthma, ulcer, heart burn etc. in recent times the plant is reported to have anticancer activities. Anti-proliferative activity of phytochemicals from this plants (as crude extract and isolated compound form) were studied on several tumor cell lines, such as, liver (HepG2) [1, 2], colon (HT29 and HCT-116) [1, 2], breast (MCF) [3, 4] and cervical cancer (U14) [5, 6] and (HeLa) [7]. Solanine (glycoalkaloid) isolated from *S. nigrum* induced caspase dependent apoptosis in HepG2 cell line following mitochondrial pathway [8]. A glycoprotein of 150kDa of this plant showed anti-proliferative activity on HCT-116 [2], HeLa [7], HT-29 [9], Hep3B [10], and MCF-7 [11] cell lines. Aqueous extract of this plant induced autophagic cell death in HEC1A, HEC1B and KLE cells [12]. Aqueous leaf extract of this plant induced autophagy and apoptosis in AU565 cells (breast cancer) in low and high concentrations respectively [13]. From our laboratory we have previously reported that chloroform fraction of methanolic extract of *S. nigrum* can induce apoptotic cell death in three cervical cancer cell lines, HeLa, SiHa and C33A [14]. In the present study we have evaluated that cell death inducing pathway and identified the bioactive molecules present in active fraction.

MATERIALS AND METHODS

Preparation of plant extract, fractionation of the extract, culture of cells and determination of IC50 doses in different cell lines was described previously [14]. With the IC50 doses, all the experiments were conducted at different time points.

Chemicals and reagents

AnnexinV-FITC/PI dual staining kit, JC1 based mitochondrial membrane potential kits were purchased from BD Biosciences. DCFDA based ROS generation kit was purchased from ABCAM. Cell culture media and common chemicals were purchased from HiMedia. Propidium iodide (PI), Hoechst 33258, propyl gallate, PCR primers and β-tubulin antibody were purchased from Sigma. First Strand cDNA synthesis kit was from Thermo Scientific. Antibodies for Bcl-2, BAX and p53 were from Santa Cruz Biotechnology where that of caspase-3, γ-H2AX were from Cell Signaling Technology. The nitrocellulose membrane was from Pall membranes and NBT-BCIP was of Invitrogen technologies.

Cellular and nuclear morphology

Cells (HeLa, SiHa and C33A) were seeded at a concentration of 5 x 10^3 cells per coverslip (pre-coated with L-Lysine) for overnight in MEM at 37 °C and 5% ĢOin a humidified atm osphere. After incubation, cells were treated with the IC_{50} doses of the extract fraction along with a control set each for 24 h. After treatment cells were briefly washed with chilled PBS, fixed with 4% PFA and washed again. Then stained with Hoechst 33258 (2µg/ml) for 2 min at room temperature, washed with PBS and mounted in mounting medium (PBS: Glycerol=1:9) containing propyl gallate.

Apoptosis assay (AnnexinV-FITC/PI double staining)

Externalization of phosphatidylserine (PS) is a well known marker of apoptosis. Annexins are a family of calcium-dependent phospholipid binding proteins which bind to PS to identify apoptotic cells. Cells (HeLa, SiHa and C33A) were seeded at a concentration of 5 x 10^5 cells per T-25 flask overnight in MEM at 37 °C and 5% CO_2 in a humidified atmosphere. After incubation, cells were treated with the IC_{50} doses of the extract fraction along with a control set each for 24 h. After treatment, cells were harvested, washed with PBS,

stained with Annexin V-FITC antibody and PI for 15 min at dark and subjected to flow cytometry (BD FACS Verse).

Cell cycle shift

Due to induction of cell death, some changes occurred in the cell cycle pattern. So the cell cycle patterns of control and treated sets were evaluated by measuring the total DNA content using flow cytometric technique. After 24hours treatment with the IC50 doses, cells were harvested, washed with PBS, fixed with 70% ethanol, treated with RNase A at 37 °C for 2 h, and then stained with PI, incubated at dark for 15 min and subjected to flowcytometry.

Gene expression study by semi Q RT-PCR

After 24 h treatment, cells were harvested and washed with PBS. Total RNA was isolated from the cells using Tri reagent (Sigma) according to manufacturer's protocol. RNA was quantified by UV spectroscopy and integrity of the RNA samples was checked by running in Agarose gels containing sodium hypochlorite [15]. Using first strand cDNA synthesis kit, cDNA was prepared taking 1µg RNA as starting material following manufacturer's protocol. 1 µl cDNA was taken to do PCRs for several apoptotic genes. GAPDH served as internal control for normalization of the cDNAs. Primers for the PCR reactions (Sigma) were designed by Primer 3 software using FASTA sequences of target genes from NCBI. The primer sequences and PCR profiles were listed in table 1.

After PCR, products were run in Agarose gels and photographed in Gel documentation system (UVP MultiDoc-It). Densitometric analysis was done by NIH-ImageJ software following NIH guidelines. Relative densities of the gene expression with respect to the non-treated sets were calculated and histograms were produced (Microsoft Excel)

Table 1: Primer sequences and PCR profiles of the genes analyzed in RT-PCR

Gene	Primer sequence (5'→ 3')						
	Forward			Reverse			
p53	ATGGCCATCTACAAGCAG			ACAGTCAAGAGCCAACCTCAG			
p21	ATGAAATTCACCCCCTTTCC			CCCTAGGCTGTGCTCACTTC			
BAX	GTGGCAGCTGACATGTTTTC			GGAGGAAGTCCAATGTCCAG			
Bcl-2	GGGTACGATAACCGGGAGAT			CTGAAGAGCTCCTCCACCAC			
ET-1	TCCTCTGCTGGTTCCTGACT			CAGAAACTCCACCCCTGTGT			
HPV16 E6	TTGCTTTTCGGGATTTATGC			CAGGACACAGTGGCTTTTGA			
HPV18 E6	TGAAAAACGACGATTCCACA			TTGTGTTTCGCGTCGTT			
GAPDH	CAAGGTCATCCATGACAACTTTG			GTCCACCACCCTGTTGCTGTAG			
	PCR profile						
	Initial denaturation (°C-min)	Denaturation (°C-s)	Annealing (°C-s)	Extension (°C-s)	Number of cycles	Final extension (°C-min)	Product length (bp)
p53	94–4	94–30	58–30	72–45	35	72–7	210
p21			57–30	72–30			174
BAX			58–30	72–45			151
Bcl-2			58–30	72–45			395
ET-1			57–30	72–45			242
HPV16 E6			52–30	72–30			106
HPV18 E6			53–30	72-30			285
GAPDH			58–30	72–45			496

Protein expression study by immunoblotting

After 24 h treatment, cells were harvested and washed in PBS. Then protein was extracted by lysing cells with 1X sample loading buffer. Total protein in the cell lysates were quantified by Lowry method and 50 µg of each sample was run in 10/12% polyacrylamide gels according to need. ß-tubulin served as the loading control. After gel run, proteins were blotted in nitrocellulose membrane (Pall-0.22 µm) and checked with Ponceu S stain. Membranes were blocked with 5% BSA for 3 h at room temperature and subsequently incubated with Primary antibody for overnight at 4 °C with gentle shaking. Then washed with TBST (Tris buffered saline with 0.05% Tween 20 buffer) and incubated with AP-conjugated secondary antibody for 3 h at room temperature. Then washed well with TBST and TBS and incubated with the substrate NBT-BCIP until bands appear. After the appearance of bands, reaction was stopped with water and photographed in gel documentation system (UVP-multidoc It). Densitometric analysis was done as described previously.

ROS generation

After 3 h treatment, cells were briefly washed with PBS and stained with H_2DCFDA for 30 min at 37 °C and then rewashed with PBS and visualized under epi-fluorescent microscope (Leica).

Loss of mitochondrial membrane potential

After 4 h treatment, cells were briefly washed with PBS and stained with JC1 for 15 min at 37 °C and rewashed with PBS and visualized under epi-fluorescent microscope (Leica).

Incorporation of γH2AX

After 6 h treatment, cells were briefly washed with PBS and fixed with 4% PFA at room temperature for 15 min, washed, incubated overnight with anti-**γ**H2AX antibody at 4 °C in a humidified container. Then washed with PBS and incubated with FITC conjugated antibody for 3 h at room temperature, rewashed with PBS, mounted in mounting medium (PBS: Glycerol=1:9) containing propyl gallate and visualized under epi-fluorescent microscope (Leica).

Column chromatography

Chloroform fraction was concentrated and mixed with silica gel (60-120) and packed in a column with silica gel (60-120). Then the column was eluted with hexane, ethyl acetate and methanol with increasing polarity. Fractions were collected, checked with TLC and pooled if necessary. Fractions were checked for their cytotoxicity by MTT assay. Positive samples were subjected to GC-MS study.

GC-MS

Samples were TMS derivatized with BSTFA (Sigma) following manufacturer's protocol and run in HP5-MS capillary column (30m X 0.25 mm X 0.25 µm) and run through a temperature gradient of 70-260 °C with a ramping rate of 5 °C per min. Fragmentation pattern of the peaks were matched with NIST library.

RESULTS

Cellular and nuclear morphology

Drastic changes in both cellular and nuclear morphology were observed in all the treated cell lines. Morphology of apoptotic features, such as cell shrinkage associated with extensive cytoplasmic blebbing was observed. Along with that, nuclear condensation and fragmentation were also visible.

Apoptotic assay (AnnexinV FITC/PI assay)

For 24 h treatment, most of the treated cells were in late apoptotic phase (fig. 2). In HeLa cells, 22.86% cells were found to be apoptotic, whereas in SiHa and C33A cells, higher percentages of cells (34.27% and 57.9% respectively) were apoptotic.

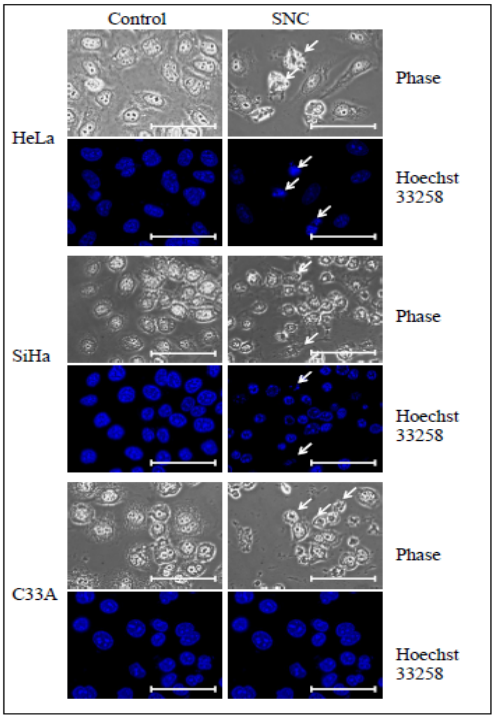

Fig. 1: Representative phase and fluorescence pictures of control and treated sets in HeLa, SiHa and C33A cells. Arrows show apoptotic features. Scale represents 50 µm

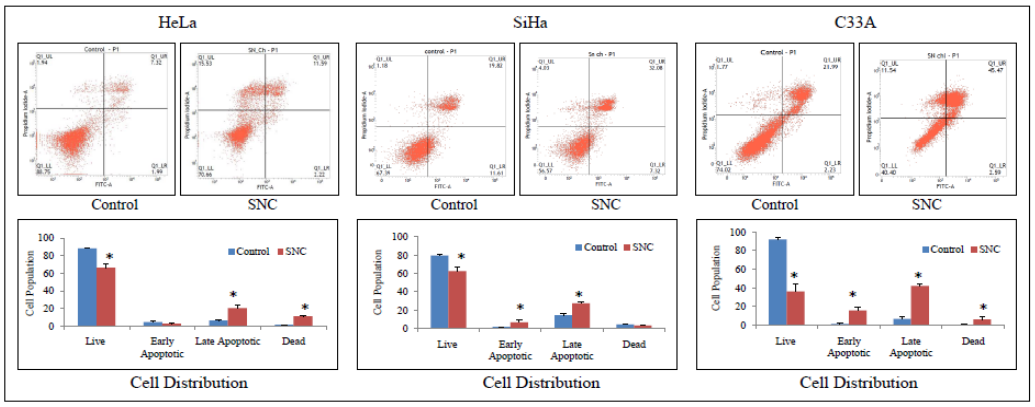

Fig. 2: Representative dot plots along with Bar graph showing cell distribution in different sets of HeLa, SiHa and C33A cells after AnnexinV-FITC/PI staining; columns represent cell populations while bars represent standard deviations. * denotes significant difference between control and treated sets (P<0.05) [One way ANOVA+Dunnet's post hoc test]

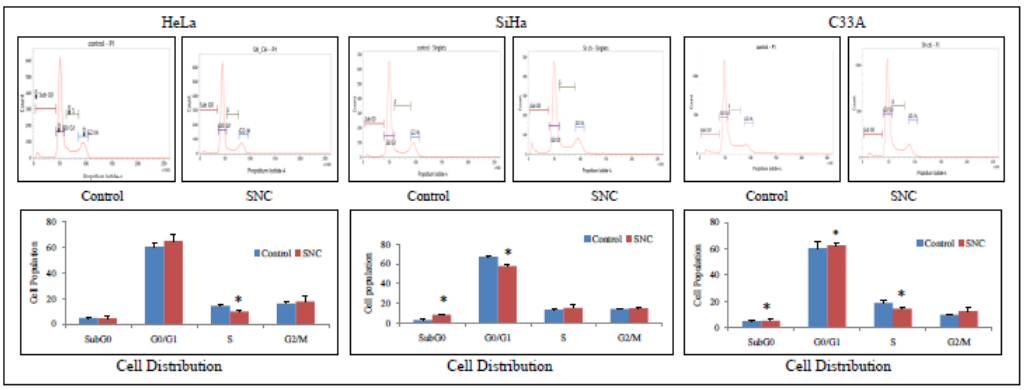

Fig. 3: Representative histograms along with Bar graph showing cell distribution in different phases of cell cycle in different sets of HeLa, SiHa and C33A cells after ethidium bromide staining; columns represent cell populations while bars represent standard deviations. * denotes significant difference between control and treated sets (P<0.05) [One way ANOVA+Dunnet's post hoc test]

Cell cycle shift

Two types of responses were observed in the cell cycle pattern of treated sets. With SNC treatment, cell cycle arrest at G1/S was observed in HeLa and C33A, whereas in SiHa, SubG0 population was found to be increased indicating greater cell death.

In HeLa cells, 4.28% increase in G0/G1 population was observed along with 4.52% decrease in S phase population, with more or less no change in G2/M and subG0 populations. In SNC treated SiHa cells, 9.23% decrease in G0G1 and 5.25% increase in sub G0 population was observed whereas, S and G2/M populations were increased slightly. In C33A cells, only 0.21% increase in sub G0 population was observed, along with 2.13% increase in G0/G1 population, 4.45% decrease in S and 2.79% increase in G2/M phase population.

Gene expression study

In all the cell lines, the treated sets had showed elevated levels of expression of pro-apoptotic genes and reduced level of anti-apoptotic genes. Expression of viral HPV 16/18 E6 gene was found to be decreased in SiHa and HeLa cells along with the decrease in expression of Endothelin-1 (ET-1).

In HeLa cells, Bcl-2 expression was decreased by 0.86 fold, while BAX expression was elevated, 0.06 fold in treated set. p53 expression was enhanced, 0.3fold while p21 expression was increased slightly (0.008fold). ET-1 expression was reduced moderately (0.11fold) and significantly in HPV E6 (0.65fold).

In SiHa cells, Bcl-2 expression was reduced by 0.43fold, but BAX, p53 and p21 expression were elevated (0.05, 0.33 and 0.12 fold respectively). ET-1 expression was reduced by 0.41fold, while E6 expression was slightly reduced, (0.12fold).

In C33A cells, surprisingly Bcl-2 expression was found to be increased slightly (0.02fold), p53 expression was increased 0.03fold, p21 was increased, 0.68fold. ET-1 expression was not detected as expected in this cell line, which didn't have HPV viral load.

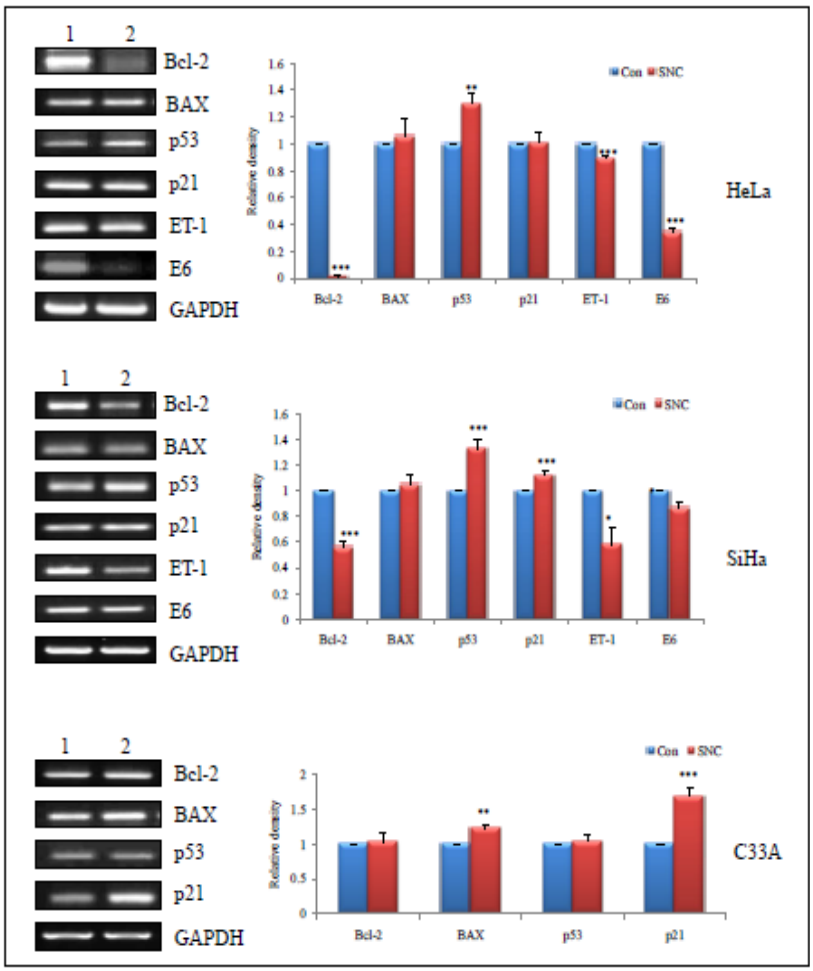

Fig. 4: Representative PCR expressions of several genes in control and treated sets in HeLa, SiHa and C33A cells [1: Control set, 2: SNC treated] along with densitometric analysis, columns represent the relative densities while bars represent standard deviations. * denotes significant difference between control and treated sets (P<0.05) [One way ANOVA+Dunnet's post hoc test]

Protein expression study

In all the cell lines, the treated sets had showed elevated levels of effecter Caspase3, pro-apoptotic BAX, p53 and reduced levels of anti-apoptotic Bcl-2 proteins.

In HeLa cells, cleaved Caspase3 was significantly increased (8.87 fold). Bcl-2 was reduced, (0.54 fold). While BAX expression was elevated, 0.17 fold. p 53 expression was elevated 0.41fold intreated set.

For SiHa cells, cleaved Caspase3 expression was elevated 0.26 fold, Bcl-2 expression was decreased by 0.08foldwhile BAX and p53 expression was increased heavily, (0.28 fold and 0.83 fold) respectively, in treated set.

In C33A cells, cleaved Caspase 3 expression was increased 1.9 fold, Bcl-2 expression decreased by 0.16 fold, BAX expression increased heavily (0.61fold) and p53 expression remained same (increased by 0.01 fold) in treated cells.

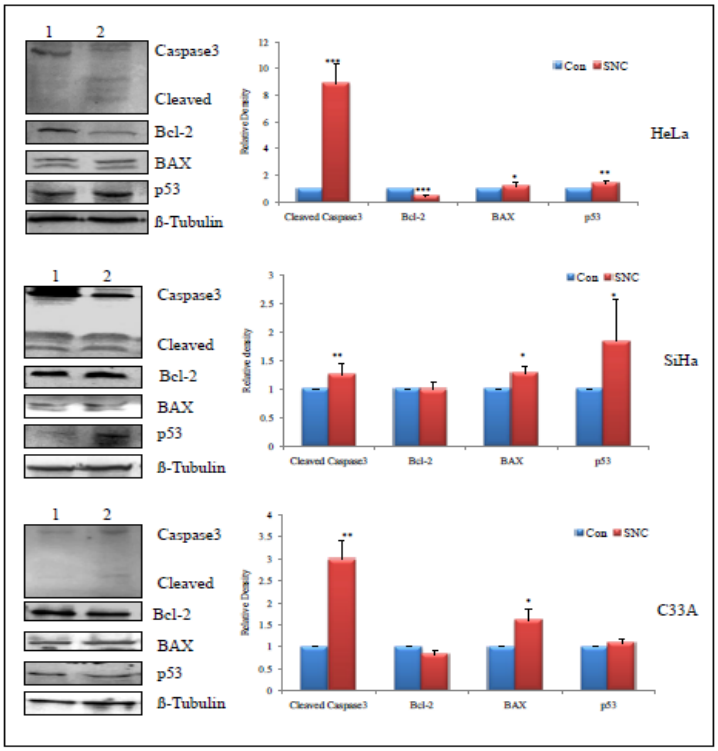

Fig. 5: Representative western blots of proteins in control and treated sets in HeLa, SiHa and C33A cells [1: Control set, 2: SNC treated] along with densitometric analysis, columns represent the relative densities while bars represent standard deviations. * denotes significant difference between control and treated sets (P<0.05) [One way ANOVA+Dunnet's post hoc test]

ROS generation

In all the treated cells, green fluorescence of DCF (formed by the oxidation of DCFDA with ROS) was detected. The effect was most pronounced in HeLa cells.

MMP assay

Loss of MMP was clearly visible. Only monomeric form of JC1 was visualized in treated sets of all cell lines.

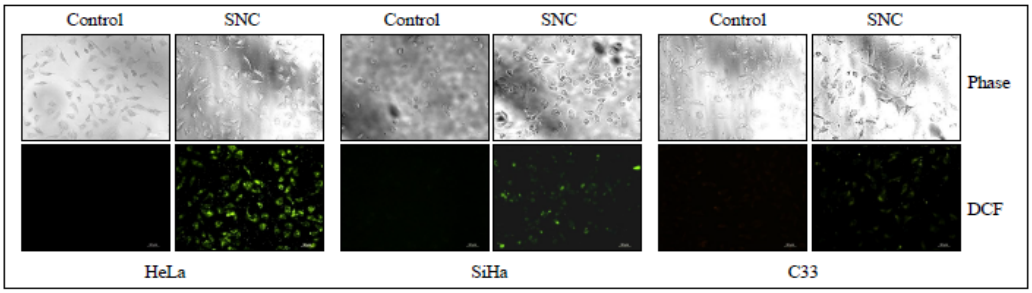

Fig. 6: Representative phase and fluorescence pictures of control and treated HeLa, SiHa and C33A cells stained with DCFDA. Scale represents 50 µm

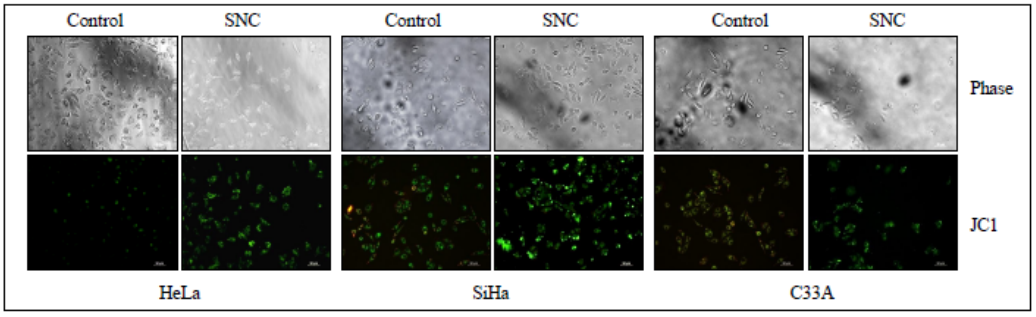

Fig. 7: Representative phase and fluorescence pictures of control and treated HeLa, SiHa and C33A cells stained with JC1. Scale represents 50 µm

Incorporation of γH2AX

For all the three cell lines, treated sets showed the presence of γ-H2AX (detected by anti γ-H2AX antibody) which is a marker of DNA damage. At 6 hours' time point this incorporation of phospho variant of H2AX clearly indicated the presence of either single or double stranded DNA damage in the treated sets.

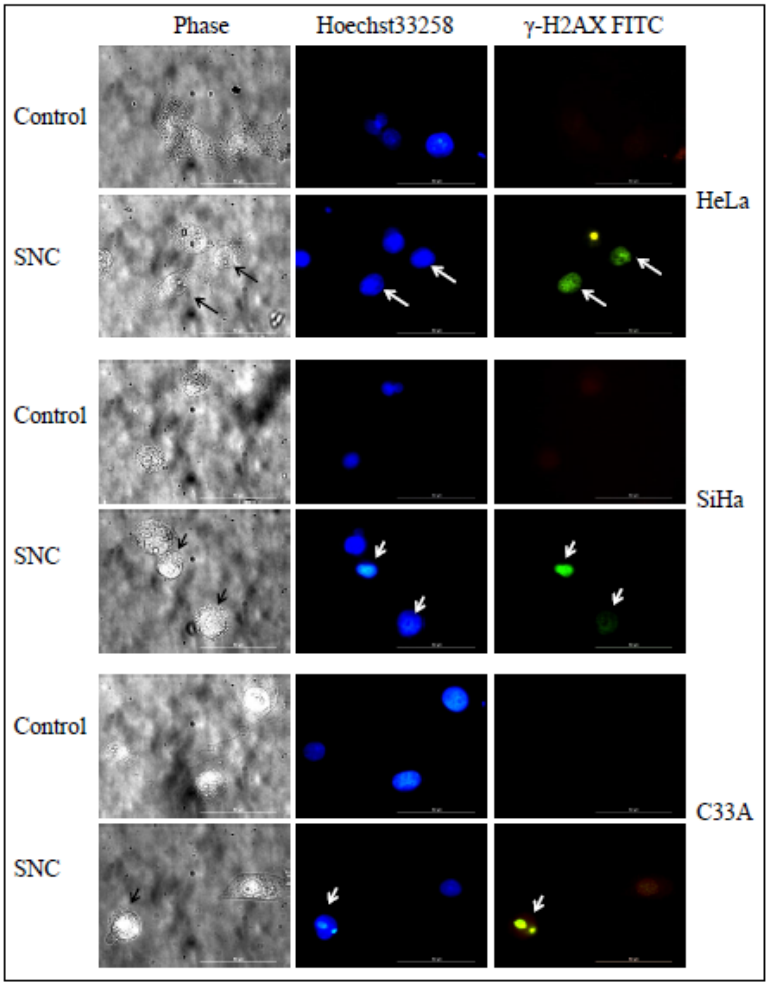

Fig. 8: Representative phase and fluorescence pictures of control and treated sets in HeLa, SiHa and C33A cells. Arrows show γ-H2AX incorporation in damaged nuclei. Scale represents 50 µm

Column chromatography and GC-MS

Several sub fractions were isolated from the chloroform fraction by column chromatography. Out of which, sub fractions (SF) 17-18, 19-20, and 21 were found to be cytotoxic by MTT assay. Common constituents of the SFs were Stearic acid TMS ester (major constituent), Phenol 2, 4-Bis (1, 1–dimethylethyl), Palmitic acid TMS ester, Butanedioic acid TMS ester.

SF17-18 had 2.42% Butanedioic acid TMS ester, 2.48% Phenol 2, 4-Bis (1, 1–dimethylethyl), 16.10% Palmitic acid TMS ester and 31.54% Stearic acid TMS ester. SF19-20 had 2.48% Butanedioic acid TMS ester, 4.21% Phenol 2, 4-Bis (1, 1–dimethylethyl), 23.12% Palmitic acid TMS ester and 31.48% Stearic acid TMS ester. SF21 had 5.96% Butanedioic acid TMS ester, 1.72% Phenol 2, 4-Bis (1, 1–dimethylethyl), 20.86% Palmitic acid TMS ester and 28.25% Stearic acid TMS ester.

DISCUSSION

Earlier workers reported anti-proliferative activity of *S. nigrum* phytochemicals on cervical cancer cells. Methanolic extract of *S. nigrum* fruit showed cytotoxicity on HeLa cells with IC50 dose of 847.8µg/ml [16] which is much higher than our observed IC50 dose of SNC (250±1.01µg/ml) for HeLa cells. For SiHa and C33A cells that was even less (87.5±0.82µg/ml and 100±0.03µg/ml). So chloroform fraction of methanolic extract of whole plant of *S. nigrum* worked better than the methanolic extract of *S. nigrum* fruits. GC-MS analysis of chloroform fraction of plant extracts (PCFs) were found to be enriched with fatty acids. Both short chained (C4-Butanedioic acid, C-7-Benzoic acid) and long chained (C18-Stearic acid, Oleic acid, Linoleic acid) fatty acids were detected in the fractions. These natural fatty acids are useful for membrane integrity and played an important role in cell signaling in plants, whereas in animal cells these compounds exhibit an array of therapeutic activities. Along with anti inflammatory and antioxidant activities, a number of unsaturated fatty acids are reported to have anticancer activities when tested on human cancer cell lines [17-20]. Saturated as well as unsaturated fatty acids were detected in the plant extracts. Phenol 2, 4-Bis (1, 1–dimethyl ethyl) was detected in SNC fraction. This compound was also detected in the bioactive (ethanolic acid) fraction of *S. trilobatum* inhibiting Elrich's Ascites Carcinoma growth [21]. Stearic acid, a C18 long chain fatty acid was also present in both the fractions reported to have inhibitory activity against cervical cancer line HOG-1 [22]. Palmitic acid present in SNC, showed selective cytotoxicity to MOLT-4 (Human leukemic) cell line, probably by inhibiting DNA topoisomerase-I [23].

With this fatty acid rich fraction, treated cells showed clear signs of late events of apoptosis. Morphological features, such as, membrane blebbing, shrinkage of cell size along with nuclear condensation and

fragmentation indicated apoptosis induction. Another late event of apoptosis was studied by AnnexinV-FITC/PI double staining, as AnnexinV protein binds to phosphatidylserine, which externalizes, as a result of membrane flipping, after apoptosis induction. In HeLa and C33A cells, the increase in G0/G1 population and decrease in S phase population indicated G1/S cell cycle arrest. Crude polysaccharides isolated from *S. nigrum* showed significant growth inhibition on cervical cancer (U14) of tumor bearing mice showing increased expression of BAX and decreased expression of Bcl-2 [24]. It was reported that Endothelin-1 (ET-1) is responsible for neoplastic growth in HPV associated carcinoma cells [25]. At the transcriptional level, expression of ET-1 was found to decrease significantly in the treated HeLa cells and slightly in the SiHa cells, which may have help in attenuating the proliferation of these cells. SNC treatment also elevated the expression of BAX and down regulated Bcl-2 in all the three cell lines. Along with that, expression of p53 was elevated in all the cells. Up regulation of p53 may occur in two ways. In one pathway, SNC mediated ROS production within the cells may results in the subsequent DNA damage which might leads to up regulation of p53. Presence of phospho loci in the treated cells also vindicated this. In the second pathway, down regulation of HPV 16/18 E6 by SNC may also help in stabilization of functional p53. p53 acted as the master regulator in this case. In one hand it increases the expression of BAX and down regulate Bcl-2, on the other hand up regulate p21 and cells were arrested at G1/S check point. With the BAX activation, subsequent loss of mitochondrial membrane potential and caspase activation took place. A probable mode of action of SNC on the cervical cancer cells is presented (fig. 9).

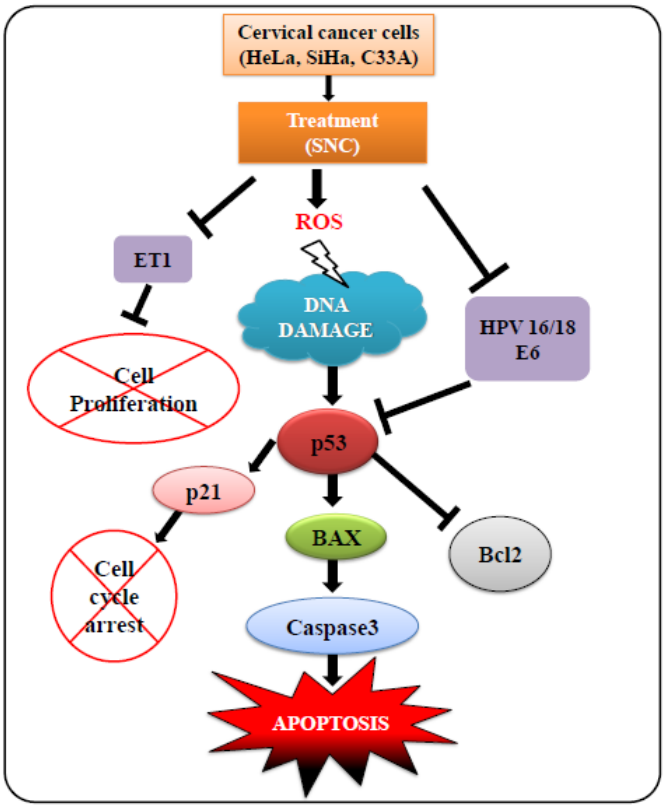

Fig. 9: Probable mode of action of the PCFs over the cell lines

CONCLUSION

From the study it can be concluded that SNC is capable of inducing apoptosis in cervical cancer cells. Induction of ROS mediated DNA damage by this chloroform fraction might have induced cell death. Presence of damaged DNA was detected in the treated cells which might be the cause of p53 up regulation along with stabilization of p53 due to HPV E6 down regulation. With down regulation of anti-apoptotic Bcl-2 and up regulation of BAX, caspase dependent apoptosis was induced following intrinsic mitochondrial pathway. The SNC fraction was rich in different fatty acids, phenolics, alkaloids which might be responsible for the apoptosis induction singly or in a synergistic way.

ACKNOWLEDGEMENT

Authors would like to thank UGC-CAS, DST-FIST, DST-PURSE, Department of Botany and CRNN, University of Calcutta for instrumentation and infrastructural support. WB-DBT is acknowledged for funding this study [595-BT (Esst)/RD-2/11]. SP would like to thank UGC, GOI for the award of research fellowships. Authors are very thankful to Dr. K. P. Dhara and Mr. D. Patra for their help in column chromatography works.

AUTHOR CONTRIBUTION

SP: Designed experiments, performed experiments, wrote manuscript.

RK: Hypothesized the study, designed experiments, supervised experiments, revised manuscript.

CONFLICT OF INTERESTS

Declared none

REFERENCES

1. Ji YB, Gao SY, Ji Cf, Zou X. Induction of apoptosis in HepG2 cells by solanine and Bcl-2 protein. J Ethnopharmacol 2008;115:194-202.
2. Lee KR, Kozukue N, Han JS, Park JH, Chang EY, Baek EJ, *et al.* Glycoalkaloids and metabolites inhibit the growth of human colon (HT29) and live (HepG2) cancer cells. J Agric Food Chem 2004;52:2832-9.
3. Leporatti ML, Ghedira K. Comparative analysis of medicinal plants used in traditional medicine in Italy and Tunisia. J Ethnobiol Ethnomed 2009;5:31.

4. Li J, Li QW, Gao DW, Han ZS, Lu WZ. Antitumor and immunomodulating effects of polysachharides isolated from *Solanum nigrum* Linne. Phytother Res 2009;23:1524-30.
5. Joo HY, Lim K, Lim KT. Phytoglucoprotein (150kDa) isolated from *Solanum nigrum*Linne has a preventive effect on dextran sodium sulfate induced colitis in A/J mouse. J Appl Toxicol 2009;29:207-13.
6. Li J, Li Q, Feng T, Li K. Aqueous extract of *Solanum nigrum* inhibit growth of cervical carcinoma (U14) via modulating immune response of tumor bearing mice and inducing apoptosis of tumor cells. Fitoterapia 2008;79:548-56.
7. Son Yu, Kim J, Lim JC, Chung Y, Chung GH, Lee JC. Ripe fruit of *Solanum nigrum* L. inhibits cell growth and induces apoptosis in MCF-7 cells. Food Chem Toxicol 2003;41:1421-8.
8. Glossman-Mitnik D. CHIH-DFT determination of the molecular structure and infrared and ultraviolet spectra of gamma-solanine. Spectrochim Acta A Mol Biomol Spectrosc 2007;66:208-11.
9. Schuler T, Qin Z, Ibe S, Noben-Trauth N, Blankenstein T. T helper cell type 1-associated and cytotoxic T lymphocyte-mediated tumor immunity is impaired in interleukin 4-deficient mice. J Exp Med 1999;189:803-10.
10. Lim KT. Glycoprotein isolated from *Solanum nigrum*L. kills HT-29 cells through apoptosis. J Med Food 2005;8:215-26.
11. Lee SJ, Lim KT. Cell death signal by glycine and proline rich plant glycoprotein is transferred from cytochrome c and nuclear factor kappa B to caspase 3 in Hep3B cells. J Nutr Biochem 2008;19-166-74.
12. Tai CJ, Wang CK, Chang JC, Lin CS, Tai CJ. Aqueous extract of *Solanum nigrum* leaf activates autophagic cell death and enhances docetaxel induced cytotoxicity in human endometrial carcinoma cells. eCAM 2012:1-10. http://dx.doi.org/ 10.1155/2012/859185
13. Huang HC, Syu KY, Lin JK. Chemical composition of *Solanum nigrum* Linn extract and induction of autophagy by leaf water extract and its major flabonoids in AU565 breast cancer cells. J Agric Food Chem 2010;58:8699-708.
14. Paul S, Chakraborty S, Mukherjee A, Kundu R. Evaluation of cytotoxicity and DNA damaging activity of three plant extracts on cervical cancer cell lines. Int J Pharm Sci Rev Res 2015;31:183-9.
15. Aranda PS, LA Joie DM, Jorcyk CM. Bleach gel: a simple agarose gel for analyzing RNA quality. Electrophoresis 2012;33:366-9.
16. Patel S, Gheewala N, Suthar A, Shah A. *In vitro* cytotoxicity activity of *Solanum nigrum* extracts against HeLa cell line and Vero cell line. Int J Pharm Pharm Sci 2009;1:38-46.
17. Chapkin RS, McMurray DN, Lupton JR. Colon cancer, fatty acids and anti inflammatory compounds. Curr Opin Gastroenterol 2007;23:48-54.
18. Lee J, Hwang DH. Dietary fatty acids and eicosanoids. In: Chow CK. editor. Fatty acids in foods and their Heath Implecations. London UK: CRC Press; 2008. p. 713-39.
19. Sakai M, Kakutani S, Horikawa C, Tokuda H, Kawashima H, Shibata H, *et al.* Arachidonic acid and cancer risk: a systemic review of observational studies. BMC Cancer 2012;12:606.
20. Tsuzuki T, Shibata A, Kawakami Y, Nakagawa K, Miyazawa T. Conjugated eicosapentaenoic acid inhibits vascular endothelial growth factor induced angiogenesis by suppressing the migration of human umbilical vein endothelial cells. J Nutr 2007;137:641-6.
21. Xavier AP, Santharam L, Panigrahi S, Muthuraman MS, Pemiah B. Antitumor potential of ethanolic extract of *Solanum tribatum*against Ehrlich's Ascites Carcinoma. Int J Pharm Tech Res 2013;5:1119-25.
22. Gleeson RP, Ayub M, Wright JT, Wood CB, Habib NA, Soutter WP, *et al.* Fatty acid control of growth of human cervical and endometrial cancer cells. Br J Cancer 1990;61:500-3.
23. Harada H, Yamashita U, Kurihara H, Fukushi E, Kawabata, Kamey Y. Antitumor activity of palmitic acid found as a selective cytotoxic substanceina marine red algae. Anticancer Res 2002;22:2587-90.
24. Li J, Li Q, Feng T, Li K. Aqueous extract of *Solanum nigrum*inhibit growth of cervical carcinoma (U14) via modulating immune response of tumor bearing mice and including apoptosis of tumor cells. Fitoterapia 2008;(7-8):548-56.
25. Venuti A, Salani D, Manni V, Poggiali F, Bagnato A. Expression of endothelin1 and endothelin A receptor in HPV associated cervical carcinoma: new potential targets for anticancer therapy. FASEB J 2000;14:2277-83.